SUPERCONVERGENCE OF THE VELOCITY IN MIMETIC FINITE DIFFERENCE METHODS ON QUADRILATERALS[*]

M. BERNDT[†], K. LIPNIKOV[†], M. SHASHKOV[†], M. F. WHEELER[‡], AND I. YOTOV[§]

Abstract. Superconvergence of the velocity is established for mimetic finite difference approximations of second-order elliptic problems over h^2-uniform quadrilateral meshes. The superconvergence result holds for a full tensor coefficient. The analysis exploits the relation between mimetic finite differences and mixed finite element methods via a special quadrature rule for computing the scalar product in the velocity space. The theoretical results are confirmed by numerical experiments.

Key words. mixed finite element, mimetic finite difference, tensor coefficient, superconvergence

AMS subject classifications. 65N06, 65N12, 65N15, 65N22, 65N30

DOI. 10.1137/040606831

1. Introduction. We consider the numerical approximation of a linear second-order elliptic problem. In porous medium applications, this equation models single phase Darcy flow and is usually written as a first-order system for the fluid pressure p and velocity $\mathbf{u}$:

$$
\begin{array}{lll}
\mathbf{u} = -\mathbf{K}\operatorname{grad} p & \text{in} & \Omega, \\
\operatorname{div} \mathbf{u} = f & \text{in} & \Omega, \\
\mathbf{u} \cdot \mathbf{n} = g & \text{on} & \partial\Omega,
\end{array}
$$

(1.1)

where $\Omega \subset \Re^2$, $\mathbf{n}$ is the outward unit normal to $\partial\Omega$, and $\mathbf{K} \in \Re^{2\times 2}$ is a symmetric uniformly positive definite full tensor representing the rock permeability divided by the fluid viscosity. We assume that system (1.1) satisfies the compatibility condition

$$
\int_\Omega f \, d\mathbf{x} + \int_{\partial\Omega} g \, ds = 0.
$$

In this paper, we analyze the convergence of a mimetic finite difference (MFD) method on quadrilateral meshes. The method uses discrete operators that preserve certain critical properties of the original continuum differential operators. Conservation laws, solution symmetries, and the fundamental identities and theorems of vector

and tensor calculus are examples of such properties. This "mimetic" technique has been applied successfully to several applications including diffusion [22, 15, 18], magnetic diffusion and electromagnetics [14], continuum mechanics [17], and gas dynamics [8]. For problem (1.1), the mimetic technique uses discrete flux $\mathcal{G}$ and divergence $\mathcal{DIV}$ operators for the continuum operators $-\mathbf{K}\mathrm{grad}$ and div, respectively, which are adjoint to each other, i.e., $\mathcal{G} = \mathcal{DIV}^*$. It is straightforward to extend the MFD method to locally refined meshes with hanging nodes [16], unstructured three-dimensional meshes composed of hexahedra, tetrahedra, and any cell type having three faces intersecting at each vertex.

A connection between the MFD method and the mixed finite element (MFE) method with Raviart–Thomas finite elements has been established in [4]. In particular, it was shown that the scalar product in the velocity space proposed in [15] for MFD methods can be viewed as a quadrature rule in the context of MFE methods. Another closely related method is the control-volume MFE method [7, 9].

MFE discretizations on quadrilateral grids have been studied in [25, 26, 2, 13]. These methods are based on the Piola transformation [25, 6], which preserves continuity of the normal component of the velocity $\mathbf{u}$ across mesh edges. Unfortunately, this results in the necessity to integrate rational functions over quadrilaterals. The task becomes even more complicated when the diffusion tensor is full and nonconstant. The results in [4] provide an efficient numerical quadrature rule with a minimal number of points. Moreover, the connection between the two methods allows for extensions of MFE methods to general polygons and polyhedra.

The aforementioned connection provides a suitable functional frame for rigorous analysis of convergence of mimetic discretizations. In [4], first-order convergence for the fluid pressure and velocity was shown. In this paper, we establish velocity superconvergence for MFD discretizations of (1.1) on h^2-uniform quadrilateral meshes (as defined in (2.2)–(2.3)). Precise calculation of the fluid velocity is important for porous media and other applications. The points or lines where the numerical solution is superclose to the exact solution may be used to improve the accuracy of the overall simulation. Various superconvergence results for MFE methods have been established for rectangular meshes [21, 19, 27, 10, 11, 12, 3, 1] and general quadrilateral meshes [2, 13].

In [13], velocity superconvergence is established for the MFE discretization of (1.1) on h^2-uniform quadrilateral grids. In this paper, we exploit the relation between MFD methods and MFE methods with the quadrature rule (3.10) to establish superconvergence for velocities in MFD discretizations. In particular, we show that the computed normal velocities are superclose to the true normal velocities at the midpoints of the edges. In [18], an alternative quadrature is introduced, which preserves symmetry of the exact solution on polar grids. This symmetry preservation is important for problems of radiation transport in the asymptotic diffusion limit. The analysis of superconvergence for symmetry-preserving quadratures is left for future investigation.

The paper outline is as follows. In section 2, we describe the MFE method for (1.1). In section 3, the MFD method is presented and related to the MFE method with a quadrature rule. The main superconvergence results are presented in section 4. Superconvergence of the normal velocities at the midpoints of the edges is established in section 5. In section 6, numerical experiments are given that confirm the theoretical results.
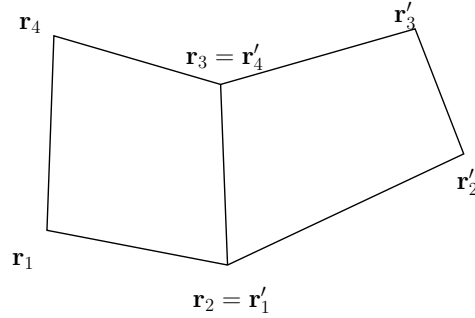
FIG. 2.1. h^2-uniform quadrilateral grid.

2. The MFE method. To simplify the exposition, we assume without loss of generality that $g = 0$, i.e., homogeneous Neumann boundary conditions are imposed on $\partial\Omega$.

Throughout this paper, we shall use the notation $\|\cdot\|_{k,D}$, $\|\cdot\|_{\mathrm{div},D}$, and $\|\cdot\|_D$ for the norms on the Hilbert spaces $H^k(D)$, $H(\mathrm{div}; D)$, and $L_2(D)$, respectively, where $D \subset \Omega$. In addition, $|\cdot|_{k,D}$ will denote the seminorm on $H^k(D)$. To simplify notation, we shall omit the subscript D when $D = \Omega$. Finally, we denote by $(\cdot, \cdot)$ the L^2-inner product on Ω of either scalar or vector functions. Let

$$\mathbf{V} = \{\mathbf{v} \in H(\mathrm{div};\Omega) : \mathbf{v}\cdot\mathbf{n} = 0 \text{ on } \partial\Omega\} \quad \text{and} \quad W = \left\{w \in L_2(\Omega) : \int_\Omega w\,d\mathbf{x} = 0\right\}.$$

The variational formulation of (1.1) is as follows: find a pair $(\mathbf{u}, p) \in \mathbf{V} \times W$ such that

$$
\begin{aligned}
(\mathbf{K}^{-1}\mathbf{u},\ \mathbf{v}) - (p,\ \mathrm{div}\ \mathbf{v}) &= 0, \\
(\mathrm{div}\ \mathbf{u},\ w) &= (f,\ w) \qquad \forall\,(\mathbf{v},\ w) \in \mathbf{V} \times W.
\end{aligned}
\tag{2.1}
$$

For the discretization of (2.1), denote by $\mathcal{T}_h$ a *shape-regular* partition (see [5, Remark 2.2, p. 113]) of $\bar{\Omega}$ into convex quadrilateral elements of diameter not greater than h. For two examples of shape-regular grids, see Figure 6.1. We assume that the grid is h^2-uniform. Following [13], the quadrilateral partition $\mathcal{T}_h$ is called h^2-uniform if each element is an h^2-parallelogram, i.e.,

$$\|(\mathbf{r}_2 - \mathbf{r}_1) - (\mathbf{r}_3 - \mathbf{r}_4)\| \le Ch^2, \tag{2.2}$$

and any two adjacent quadrilaterals form an h^2-parallelogram, i.e.,

$$\|(\mathbf{r}_2 - \mathbf{r}_1) - (\mathbf{r}_2' - \mathbf{r}_1')\| \le Ch^2, \tag{2.3}$$

where $\mathbf{r}_1'$, $\mathbf{r}_2'$, $\mathbf{r}_3'$, and $\mathbf{r}_4'$ are the vertices of the adjacent element (see Figure 2.1).

For any convex quadrilateral e, there exists a bijection mapping $\mathbf{F}_e : \hat{e} \to e$, where $\hat{e}$ is the reference unit square with vertices $\hat{\mathbf{r}}_1 = (0, 0)^T$, $\hat{\mathbf{r}}_2 = (1, 0)^T$, $\hat{\mathbf{r}}_3 = (1, 1)^T$, and $\hat{\mathbf{r}}_4 = (0, 1)^T$. Denote by $\mathbf{r}_i = (x_i, y_i)^T$, $i = 1, 2, 3, 4$, the four corresponding vertices of element e as shown in Figure 2.2. Then, $\mathbf{F}_e$ is the bilinear mapping given by

$$\mathbf{F}_e(\hat{\mathbf{r}}) = \mathbf{r}_1\,(1 - \hat{x})(1 - \hat{y}) + \mathbf{r}_2\,\hat{x}(1 - \hat{y}) + \mathbf{r}_3\,\hat{x}\hat{y} + \mathbf{r}_4\,(1 - \hat{x})\hat{y}. \tag{2.4}$$
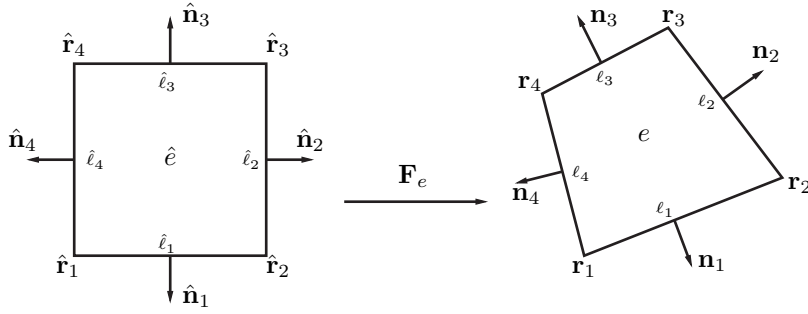
FIG. 2.2. *Bilinear mapping and orientation of normal vectors.*

Note that the Jacobi matrix $\mathbf{DF}_e$ and its Jacobian J_e are linear functions of $\hat{x}$ and $\hat{y}$. Indeed, straightforward computations yield

$$(2.5) \qquad \mathbf{DF}_e = [(1 - \hat{y})\,\mathbf{r}_{21} + \hat{y}\,\mathbf{r}_{34}, \;\; (1 - \hat{x})\,\mathbf{r}_{41} + \hat{x}\,\mathbf{r}_{32}]$$

and

$$(2.6) \qquad J_e = 2|T_{124}| + 2(|T_{123}| - |T_{124}|)\hat{x} + 2(|T_{134}| - |T_{124}|)\hat{y},$$

where $\mathbf{r}_{ij} = \mathbf{r}_i - \mathbf{r}_j$ and $|T_{ijk}|$ is the area of the triangle with vertices $\mathbf{r}_i$, $\mathbf{r}_j$, and $\mathbf{r}_k$. Since e is convex, the Jacobian J_e is always positive, i.e., $J_e > 0$.

Let ℓ_i and $\hat{\ell}_i$, $i = 1, 2, 3, 4$, be the edges of e and $\hat{e}$, respectively. Let $\mathbf{n}_i$ and $\hat{\mathbf{n}}_i$ be the unit outward normal vectors to ℓ_i and $\hat{\ell}_i$, respectively (see Figure 2.2). Similarly, let $\boldsymbol{\tau}_i$ and $\hat{\boldsymbol{\tau}}_i$ be the unit tangential vectors to ℓ_i and $\hat{\ell}_i$, respectively. It is easy to see from (2.5) that for any edge ℓ_i,

$$(2.7) \qquad \mathbf{n}_i = \frac{1}{|\ell_i|} J_e \mathbf{DF}_e^{-T} \hat{\mathbf{n}}_i \qquad \text{and} \qquad \boldsymbol{\tau}_i = \frac{1}{|\ell_i|} \mathbf{DF}_e \hat{\boldsymbol{\tau}}_i.$$

The reader is referred to [6] for suitable choices for the pair of finite element spaces $\mathbf{V}^h \subset \mathbf{V}$ and $W^h \subset W$. In this paper, we consider the lowest-order Raviart–Thomas finite element spaces RT_0 [25, 20] defined on the reference element $\hat{e}$ as

$$\hat{\mathbf{V}}(\hat{e}) = P_{1,0}(\hat{e}) \times P_{0,1}(\hat{e}), \qquad \hat{W}(\hat{e}) = P_0(\hat{e}),$$

where $P_{1,0}$ (or $P_{0,1}$) denotes the space of polynomials linear in the $\hat{x}$ (or $\hat{y}$) variable and constant in the other variable, and P_0 denotes the space of constant functions. The velocity space on any convex quadrilateral e is defined through the Piola transformation [6]

$$\frac{1}{J_e} \mathbf{DF}_e : L_2(\hat{e}) \times L_2(\hat{e}) \rightarrow L_2(e) \times L_2(e) \qquad \forall e \in \mathcal{T}_h.$$

The RT_0 spaces on $\mathcal{T}_h$ are given by

$$(2.8) \qquad \begin{aligned} \mathbf{V}^h &= \{\mathbf{v} \in \mathbf{V} \;:\; \mathbf{v}|_e = J_e^{-1} \mathbf{DF}_e \hat{\mathbf{v}} \circ \mathbf{F}_e^{-1}, \; \hat{\mathbf{v}} \in \hat{\mathbf{V}}(\hat{e}) \quad \forall e \in \mathcal{T}_h\}, \\ W^h &= \{w \in W \;:\; w|_e = \hat{w} \circ \mathbf{F}_e^{-1}, \; \hat{w} \in \hat{W}(\hat{e}) \quad \forall e \in \mathcal{T}_h\}. \end{aligned}$$

Two properties of Piola's transformation will be important in our analysis. For any $\hat{\mathbf{v}} \in \hat{\mathbf{V}}(\hat{e})$ and the related $\mathbf{v} = J_e^{-1} \mathbf{DF}_e \hat{\mathbf{v}} \circ \mathbf{F}_e^{-1}$,

$$(2.9) \qquad J_e \mathrm{div}\, \mathbf{v} = \widehat{\mathrm{div}}\, \hat{\mathbf{v}} \qquad \text{and} \qquad |\ell_i|\, \mathbf{v} \cdot \mathbf{n}_i = \hat{\mathbf{v}} \cdot \hat{\mathbf{n}}_i.$$

Note that since $\mathbf{V}^h \subset H(\mathrm{div}; \Omega)$, any vector in $\mathbf{V}^h$ has continuous normal components on the edges. A function in W^h is uniquely determined by its values at the cell-centers and a vector in $\mathbf{V}^h$ is uniquely determined by its normal components on the edges. Therefore, $\dim W^h = N_p$ and $\dim \mathbf{V}^h = N_e$, where N_p is the number of elements and N_e is the number of interior edges. Let $\{\psi_i^h\}$, $i = 1, N_p$, be a basis for W^h such that

$$\psi_i^h(c_j) = \delta_{ij} \equiv \begin{cases} 1, & i = j, \\ 0, & i \neq j, \end{cases}$$

where c_j is the center of element e_j, $j = 1, N_p$. Similarly, let ϕ_i^h, $i = 1, N_e$, be a basis for $\mathbf{V}^h$ such that $\phi_i^h \cdot \mathbf{n}_j = \delta_{ij}$, where $\mathbf{n}_j$ is a fixed unit normal vector on edge ℓ_j, $j = 1, N_e$. In order to simplify notation, we use the same way for global and local indexing of mesh edges and corresponding normal vectors.

Given the finite element spaces $\mathbf{V}^h$ and W^h, we define the discrete problem: find $(\mathbf{u}^h, p^h) \in \mathbf{V}^h \times W^h$ such that

$$\begin{aligned}
(2.10) \quad & (\mathbf{K}^{-1}\mathbf{u}^h, \mathbf{v}^h)_h - (p^h, \mathrm{div}\ \mathbf{v}^h) = 0, \\
& (\mathrm{div}\ \mathbf{u}^h, w^h) = (f, w^h) \qquad \forall (\mathbf{v}^h, w^h) \in \mathbf{V}^h \times W^h,
\end{aligned}$$

where $(\cdot, \cdot)_h$ is a continuous bilinear form corresponding to the application of a numerical quadrature rule for computing $(\cdot, \cdot)$. A detailed discussion of this quadrature rule is given in section 3.

3. MFD discretizations. In this section, we derive an MFD discretization of (1.1) and show its connection with the MFE method (2.10).

The *first* step in the mimetic technique is to specify discrete degrees of freedom for pressure and velocity. The discrete pressure unknowns are defined at the centers of the quadrilaterals, one unknown per mesh cell. The discrete velocities are defined at the midpoints of mesh edges as normal components. In other words, an edge-based unknown is a scalar and represents the orthogonal projection of a velocity vector onto the unit vector $\mathbf{n}_i$ normal to the mesh edge ℓ_i.

The *second* step in the mimetic technique is to equip the spaces of discrete pressures and velocities with scalar products. We denote the vector space of cell-centered pressures by Q^d. The dimension of Q^d equals the number of mesh cells N_p. The scalar product on the vector space Q^d is given by

$$(3.1) \qquad [p^d, q^d]_{Q^d} = \sum_{i=1}^{N_p} |e_i| \, p_i^d \, q_i^d \qquad \forall p^d, \ q^d \in Q^d,$$

where $|e_i|$ denotes the area of cell e_i and p_i^d, q_i^d are cell-centered pressure components.

It is easy to see that the vector space Q^d is isometric to the MFE space W^h in (2.8). Indeed, for any $p^h \in W^h$, there exists a unique $p^d = (p_1^d, p_2^d, \ldots, p_{N_p}^d)^T \in Q^d$ such that $p^h = \sum_{i=1}^{N_p} p_i^d \psi_i^h$ and

$$(p^h, q^h) = [p^d, q^d]_{Q^d}.$$

Note that the discrete MFD pressure variable, p_i^d, corresponds to the value of the MFE pressure function at the cell-center, $p^h(c_i)$.

We denote the vector space of edge-based velocities by X^d. The dimension of X^d equals the number of interior mesh edges N_e. The scalar product on X^d is given by

$$(3.2) \qquad [\mathbf{u}^d, \mathbf{v}^d]_{X^d} = \sum_{e \in \mathcal{T}_h} [\mathbf{u}^d, \mathbf{v}^d]_{X^d,e},$$

where $[\mathbf{u}^d, \mathbf{v}^d]_{X^d,e}$ is a scalar product over cell e involving only the normal velocity components on cell edges. Recall that a velocity vector can be recovered from two orthogonal projections on any two noncollinear vectors. Since the mesh cell is convex, any pair of normal vectors to edges with a common point satisfies the above requirement. The orthogonal projections are exactly the degrees of freedom associated with cell edges. As shown in Figure 3.1, four recovered velocity vectors can be associated with the four vertices of the quadrilateral. For example, velocity $\mathbf{v}_1$ is recovered from its projections onto the normal vectors $\mathbf{n}_1$ and $\mathbf{n}_2$. For a general quadrilateral e, we denote by $\mathbf{v}^d(\mathbf{r}_j)$ the velocity recovered at jth vertex $\mathbf{r}_j$, $j = 1, 2, 3, 4$. Then, the cell-based scalar product is given by

$$(3.3) \qquad [\mathbf{u}^d, \mathbf{v}^d]_{X^d,e} = \frac{1}{2} \sum_{j=1}^{4} |T_j| \mathbf{K}^{-1}(\mathbf{r}_j) \mathbf{u}^d(\mathbf{r}_j) \cdot \mathbf{v}^d(\mathbf{r}_j),$$

where $|T_j|$ is the area of the triangle with vertices $\mathbf{r}_{j-1}$, $\mathbf{r}_j$, and $\mathbf{r}_{j+1}$ (see Figures 2.2 and 3.1). For example, triangles T_1 and T_4 are the shaded triangles in Figure 3.1. Note that (3.3) is indeed an inner product, since $\mathbf{K}$ is a symmetric and positive definite tensor and

$$(3.4) \qquad [\mathbf{v}^d, \mathbf{v}^d]_{X^d} \geq C|||\mathbf{v}^d|||^2,$$

where $||| \cdot |||$ is the Euclidean vector norm.
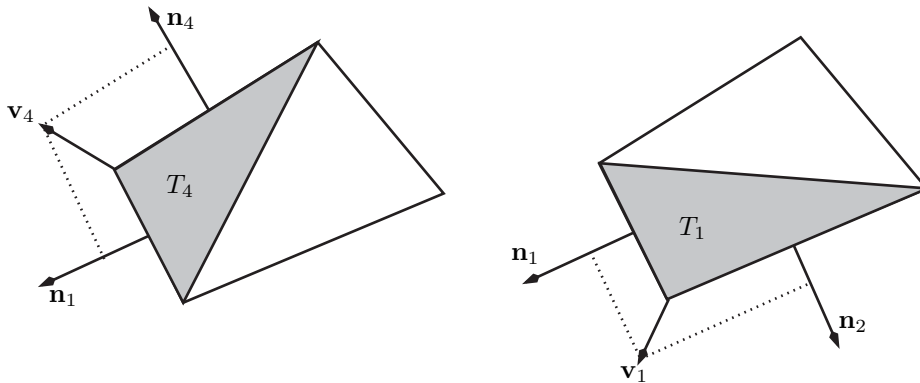
FIG. 3.1. *Recovered vectors $\mathbf{v}_1$, $\mathbf{v}_4$ and triangles T_1, T_4.*

The vector space X^d is isomorphic to the MFE space $\mathbf{V}^h$ in (2.8), since both spaces have the same definitions of degrees of freedom. In particular, for any $\mathbf{v}^h \in \mathbf{V}^h$, there exists a unique $\mathbf{v}^d = (v_1^d, v_2^d, \ldots, v_{N^e}^d)^T \in X^d$ such that $\mathbf{v}^h = \sum_{i=1}^{N_e} v_i^d \phi_i^h$. Note that the discrete MFD velocity variable, v_i^d, corresponds to the MFE normal velocity component, $\mathbf{v}^h \cdot \mathbf{n}_i$, on edge ℓ_i.

The *third* step in the mimetic technique is to derive a discrete approximation to the divergence operator, $\mathcal{DIV} : X^d \to Q^d$, which we shall refer to as the *prime*

operator. For a cell e, the Gauss divergence theorem gives

$$(3.5) \qquad \mathcal{DIV}\, \mathbf{u}^d|_e = \frac{1}{|e|} \left(u_1^d |\ell_1| + u_2^d |\ell_2| + u_3^d |\ell_3| + u_4^d |\ell_4| \right),$$

where $u_1^d, \dots, u_4^d$ are the normal velocity components on element e and the normal vectors are oriented as shown in Figure 2.2.

The *fourth* step in the mimetic technique is to derive a discrete flux operator $\mathcal{G}$ (for the continuous operator $-\mathbf{K}\mathrm{grad}$) adjoint to the discrete divergence operator $\mathcal{DIV}$ with respect to scalar products (3.1) and (3.2), i.e.,

$$[\mathcal{DIV}\mathbf{u}^d,\, p^d]_{Q^d} \equiv [\mathbf{u}^d,\, \mathcal{G}p^d]_{X^d} \qquad \forall \mathbf{u}^d \in X^d \qquad \forall p^d \in Q^d.$$

To derive the explicit formula for $\mathcal{G}$, we consider an auxiliary scalar product $\langle \cdot, \cdot \rangle$ and relate it to scalar products (3.1) and (3.2). Denote by $\langle \cdot, \cdot \rangle$ the standard vector dot product. Then

$$[p^d,\, q^d]_{Q^d} = \langle \mathcal{D}p^d,\, q^d \rangle \qquad \text{and} \qquad [\mathbf{u}^d,\, \mathbf{v}^d]_{X^d} = \langle \mathcal{M}\mathbf{u}^d,\, \mathbf{v}^d \rangle,$$

where $\mathcal{D}$ is a diagonal matrix, $\mathcal{D} = \mathrm{diag}\{|e_1|, \dots, |e_{N_p}|\}$, and $\mathcal{M}$ is a sparse symmetric mass matrix with a 5-point stencil. Restricted to a cell, this stencil connects edge-based unknowns if and only if the corresponding edges have a common point. Combining the last two formulae, we get

$$\begin{aligned}[\mathbf{u}^d,\, \mathcal{DIV}^* p^d]_{X^d} &= \langle \mathbf{u}^d,\, \mathcal{M}\,\mathcal{DIV}^* p^d \rangle = [\mathcal{DIV}\mathbf{u}^d,\, p^d]_{Q^d} \\ &= \langle \mathbf{u}^d,\, \mathcal{DIV}^t \mathcal{D}\, p^d \rangle \qquad \forall \mathbf{u}^d \in X^d \quad \forall p^d \in Q^d, \end{aligned}$$

where $\mathcal{DIV}^t$ is the adjoint of $\mathcal{DIV}$ with respect to the auxiliary scalar product. Therefore,

$$(3.6) \qquad \mathcal{G} = \mathcal{M}^{-1} \mathcal{DIV}^t \mathcal{D}.$$

The MFD method approximating first-order system (1.1) may be summarized as follows:

$$(3.7) \qquad \mathbf{u}^d = \mathcal{G}\, p^d, \qquad \mathcal{DIV}\, \mathbf{u}^d = f^d,$$

where $f^d = (f_1^d, \dots, f_{N_p}^d)^t$, and entry f_i^d is the integral average of f over cell e_i.

The basic tool for the error analysis of the discrete solution $(\mathbf{u}^d,\, p^d) \in X^d \times Q^d$ is based on the following transformation. Multiplying the first equation in (3.7) by $\mathcal{M}\mathbf{v}^d$ and the second one by $\mathcal{D}q^d$, we get

$$(3.8) \qquad \begin{aligned} [\mathbf{u}^d,\, \mathbf{v}^d]_{X^d} - [p^d,\, \mathcal{DIV}\, \mathbf{v}^d]_{Q^d} &= 0, \\ [q^d,\, \mathcal{DIV}\, \mathbf{u}^d]_{Q^d} &= [f^d,\, q^d]_{Q^d} \qquad \forall (\mathbf{v}^d, q^d) \in X^d \times Q^d. \end{aligned}$$

Using the isomorphism between the finite element space $\mathbf{V}^h \times W^h$ and the vector space $X^d \times Q^d$, we define finite element functions p^h, q^h, f^h, $\mathbf{u}^h$, and $\mathbf{v}^h$ corresponding to vectors p^d, q^d, f^d, $\mathbf{u}^d$, and $\mathbf{v}^d$, respectively. Then

$$[p^d,\, \mathcal{DIV}\, \mathbf{v}^d]_{Q^d} = (p^h, \mathrm{div}\, \mathbf{v}^h) \qquad \text{and} \qquad [q^d,\, \mathcal{DIV}\, \mathbf{u}^d]_{Q^d} = (q^h, \mathrm{div}\, \mathbf{u}^h).$$

The definition of f^d implies that

$$[f^d,\, q^d]_{Q^d} = (f^h,\, q^h) = (f,\, q^h).$$

Finally, by introducing the quadrature rule

$$(3.9) \qquad (\mathbf{K}^{-1}\mathbf{u}^h, \mathbf{v}^h)_h \equiv [\mathbf{u}^d, \mathbf{v}^d]_{X^d},$$

we reduce problem (3.7) to the finite element problem (2.10).

The scalar product in the space of velocities given by (3.3) is obviously not unique. In the context of MFE methods, it is a quadrature rule for numerical integration of $(\mathbf{K}^{-1}\mathbf{u}^h, \mathbf{v}^h)$:

$$(3.10) \qquad (\mathbf{K}^{-1}\mathbf{u}^h, \mathbf{v}^h)_{h,e} = \frac{1}{2}\sum_{j=1}^{4} |T_j| \, \mathbf{K}^{-1}(\mathbf{r}_j)\mathbf{u}^h(\mathbf{r}_j) \cdot \mathbf{v}^h(\mathbf{r}_j),$$

where $\mathbf{u}^h(\mathbf{r}_j)$ is the recovered velocity at vertex $\mathbf{r}_j$. In the context of MFE methods, we shall refer to (3.10) as the MFD quadrature rule. The global scalar product is obtained by summing over quadrilaterals, i.e.,

$$(3.11) \qquad (\mathbf{K}^{-1}\mathbf{u}^h, \mathbf{v}^h)_h = \sum_{e \in \mathcal{T}_h} (\mathbf{K}^{-1}\mathbf{u}^h, \mathbf{v}^h)_{h,e}.$$

Note that (3.4) implies that there exists a constant $C_0 > 0$ such that

$$(3.12) \qquad (\mathbf{K}^{-1}\mathbf{v}^h, \mathbf{v}^h)_h \geq C_0 \|\mathbf{v}^h\|^2 \qquad \forall \mathbf{v}^h \in \mathbf{V}^h.$$

It was shown in [4] that the element quadrature rule (3.10) is exact for any constant vector $\mathbf{u}^h$, constant tensor $\mathbf{K}$, and $\mathbf{v}^h \in \mathbf{V}^h$.

4. Superconvergence estimates for the velocity. We begin by recalling the mixed projection operator $\Pi : H^1(\Omega) \times H^1(\Omega) \to \mathbf{V}^h$ satisfying

$$(4.1) \qquad (\operatorname{div}(\Pi\mathbf{v} - \mathbf{v}), w) = 0 \qquad \forall w \in W^h.$$

The operator Π is defined locally on each element e by

$$\widehat{\Pi\mathbf{v}} = \hat{\Pi}\hat{\mathbf{v}},$$

where $\hat{\Pi} : H^1(\hat{e}) \times H^1(\hat{e}) \to \hat{\mathbf{V}}(\hat{e})$ is the reference element projection operator satisfying

$$(4.2) \qquad \int_{\hat{\ell}_i} (\hat{\Pi}\hat{\mathbf{v}} - \hat{\mathbf{v}}) \cdot \hat{\mathbf{n}}_i = 0, \quad i = 1, 2, 3, 4.$$

The approximation properties of Π have been established in [25, 26]:

$$(4.3) \qquad \|\Pi\mathbf{v}\|_{\operatorname{div}} \leq C\|\mathbf{v}\|_1,$$

$$(4.4) \qquad \|\Pi\mathbf{v} - \mathbf{v}\| \leq Ch\|\mathbf{v}\|_1,$$

$$(4.5) \qquad \|\operatorname{div}(\Pi\mathbf{v} - \mathbf{v})\| \leq Ch\|\mathbf{v}\|_2.$$

The following lemma gives several approximation properties of $\hat{\Pi}$ which will be used in the analysis.

LEMMA 4.1. *The operator $\hat{\Pi}$ defined in (4.2) satisfies, for any $\hat{\mathbf{v}} = (\hat{v}_1, \hat{v}_2)$ in $H^1(\hat{e}) \times H^1(\hat{e})$, the following:*

$$(4.6) \qquad \int_{\hat{e}} \frac{\partial}{\partial \hat{x}}(\hat{\Pi}\hat{\mathbf{v}} - \hat{\mathbf{v}})_1 \, d\hat{x}\, d\hat{y} = 0, \quad \int_{\hat{e}} \frac{\partial}{\partial \hat{y}}(\hat{\Pi}\hat{\mathbf{v}} - \hat{\mathbf{v}})_2 \, d\hat{x}\, d\hat{y} = 0,$$

$$(4.7) \qquad \left\|\frac{\partial}{\partial \hat{x}}(\hat{\Pi}\hat{\mathbf{v}})_1\right\|_{\hat{e}} \leq C\left\|\frac{\partial}{\partial \hat{x}}\hat{v}_1\right\|_{\hat{e}}, \quad \left\|\frac{\partial}{\partial \hat{y}}(\hat{\Pi}\hat{\mathbf{v}})_2\right\|_{\hat{e}} \leq C\left\|\frac{\partial}{\partial \hat{y}}\hat{v}_2\right\|_{\hat{e}},$$

$$(4.8) \qquad \|\hat{\Pi}\hat{\mathbf{v}}\|_{1,\hat{e}} \leq C\|\hat{\mathbf{v}}\|_{1,\hat{e}}.$$

Proof. The identities in (4.6) follow easily from definition (4.2). In particular, writing (4.2) for the two vertical edges gives

$$\int_0^1 (\hat{\Pi}\hat{\mathbf{v}} - \hat{\mathbf{v}})_1(0, \hat{y}) \, d\hat{y} = 0, \quad \int_0^1 (\hat{\Pi}\hat{\mathbf{v}} - \hat{\mathbf{v}})_1(1, \hat{y}) \, d\hat{y} = 0.$$

Subtracting the above equations and applying the fundamental theorem of calculus implies the first identity in (4.6). The proof of the second identity is similar. Note that (4.6) means that $\frac{\partial}{\partial \hat{x}}(\hat{\Pi}\hat{\mathbf{v}})_1$ and $\frac{\partial}{\partial \hat{y}}(\hat{\Pi}\hat{\mathbf{v}})_2$ are the L^2-orthogonal projections of $\frac{\partial}{\partial \hat{x}}\hat{v}_1$ and $\frac{\partial}{\partial \hat{y}}\hat{v}_2$, respectively, onto the space of constants, which implies (4.7). Finally, it is easy to see that (4.2) implies

$$\|\hat{\Pi}\hat{\mathbf{v}}\|_{\hat{e}} \leq C\|\hat{\mathbf{v}}\|_{1,\hat{e}},$$

which, combined with (4.7), gives (4.8).   □

We also make use of the L^2-projection operator $P_h : W \to W^h$ such that for $p \in W$,

$$(4.9) \qquad (P_h \, p - p, \, w) = 0 \qquad \forall w \in W^h.$$

Denote the quadrature error by

$$(4.10) \qquad \sigma(\mathbf{q}, \mathbf{v}) \equiv (\mathbf{q}, \mathbf{v}) - (\mathbf{q}, \mathbf{v})_h.$$

The variational formulation (2.1) and the discrete problem (2.10) give rise to the error equations

$$(4.11) \quad \begin{aligned} (\mathbf{K}^{-1}(\Pi\mathbf{u} - \mathbf{u}^h), \mathbf{v}^h)_h &= (P_h p - p^h, \operatorname{div} \mathbf{v}^h) \\ &\quad + (\mathbf{K}^{-1}(\Pi\mathbf{u} - \mathbf{u}), \mathbf{v}^h) - \sigma(\mathbf{K}^{-1}\Pi\mathbf{u}, \mathbf{v}^h), \\ (\operatorname{div}(\Pi\mathbf{u} - \mathbf{u}^h), w^h) &= 0, \end{aligned}$$

where we used (4.9) and (4.1) in the first and second equations, respectively. We note that, using (2.9), the second equation in (4.11) gives

$$0 = (\operatorname{div}(\Pi\mathbf{u} - \mathbf{u}^h), w^h)_e = (\widehat{\operatorname{div}}(\hat{\Pi}\hat{\mathbf{u}} - \hat{\mathbf{u}}^h), \hat{w}^h)_{\hat{e}} \qquad \forall w^h \in W_h.$$

Since $\widehat{\operatorname{div}}\,\hat{\mathbf{V}}^h = \hat{W}_h$, taking $\hat{w}^h = \widehat{\operatorname{div}}(\hat{\Pi}\hat{\mathbf{u}} - \hat{\mathbf{u}}^h)$ implies that $\widehat{\operatorname{div}}(\hat{\Pi}\hat{\mathbf{u}} - \hat{\mathbf{u}}^h) = 0$ and therefore, by (2.9),

$$(4.12) \qquad \operatorname{div}(\Pi\mathbf{u} - \mathbf{u}^h) = 0.$$

Taking $\mathbf{v}^h = \Pi\mathbf{u} - \mathbf{u}^h \in \mathbf{V}^h$ and $w^h = P_h p - p^h$ in (4.11) gives

$$(4.13)$$
$$(\mathbf{K}^{-1}(\Pi\mathbf{u} - \mathbf{u}^h), \Pi\mathbf{u} - \mathbf{u}^h)_h = (\mathbf{K}^{-1}(\Pi\mathbf{u} - \mathbf{u}), \Pi\mathbf{u} - \mathbf{u}^h) - \sigma(\mathbf{K}^{-1}\Pi\mathbf{u}, \Pi\mathbf{u} - \mathbf{u}^h).$$

The estimate for the first term on the right-hand side of (4.13) follows from Theorem 5.1 in [13] and (4.12):

$$(4.14) \quad \begin{aligned} (\mathbf{K}^{-1}&(\Pi\mathbf{u} - \mathbf{u}), \Pi\mathbf{u} - \mathbf{u}^h) \\ &\leq C\, h^2 \left(\|\mathbf{u}\|_2 \|\Pi\mathbf{u} - \mathbf{u}^h\| + \|\mathbf{u}\|_1 \|\operatorname{div}(\Pi\mathbf{u} - \mathbf{u}^h)\|\right) \\ &= C\, h^2 \|\mathbf{u}\|_2 \, \|\Pi\mathbf{u} - \mathbf{u}^h\|. \end{aligned}$$

The second term on the right-hand side of (4.13) can be bounded using Lemma 4.3:

$$
(4.15) \qquad |\sigma(\mathbf{K}^{-1}\Pi\mathbf{u}, \Pi\mathbf{u} - \mathbf{u}^h)| \le C\, h^2 \|\mathbf{u}\|_2 \|\Pi\mathbf{u} - \mathbf{u}^h\|.
$$

Combining (4.14), (4.15), and (3.12), we obtain the following superconvergence result.

THEOREM 4.2. *Let* $\mathbf{K}^{-1} \in W^{2,\infty}(\Omega)$. *For the velocity* $\mathbf{u}^h$ *of the MFE method* (2.1), *on* h^2-*uniform quadrilateral grids, there exists a positive constant* C *independent of* h *such that*

$$
(4.16) \qquad \|\Pi\mathbf{u} - \mathbf{u}^h\| \le C\, h^2 \|\mathbf{u}\|_2.
$$

We now proceed to prove estimate (4.15).

LEMMA 4.3. *Let* $\mathbf{v} \in \mathbf{V}^h$, *and let* $\mathbf{K}^{-1} \in W^{2,\infty}(\Omega)$. *There exists a positive constant* C *independent of* h *such that*

$$
(4.17) \qquad |\sigma(\mathbf{K}^{-1}\Pi\mathbf{u}, \mathbf{v})| \le C\, h^2 (\|\mathbf{u}\|_2\, \|\mathbf{v}\| + \|\mathbf{u}\|_1 \|\mathrm{div}\, \mathbf{v}\|).
$$

Proof. For an element $e \in \mathcal{T}^h$, we define the error

$$
(4.18) \qquad \sigma_e(\mathbf{K}^{-1}\Pi\mathbf{u}, \mathbf{v}) = \int_e \mathbf{K}^{-1}\Pi\mathbf{u} \cdot \mathbf{v}\, d\mathbf{x} - (\mathbf{K}^{-1}\Pi\mathbf{u}, \mathbf{v})_{h,e}.
$$

With (3.10), the second term on the right-hand side of (4.18) can be written as

(4.19)

$$
\begin{aligned}
(\mathbf{K}^{-1}\Pi\mathbf{u}, \mathbf{v})_{h,e} &= \frac{1}{2} \sum_{j=1}^{4} |T_j| \mathbf{K}^{-1}(\mathbf{r}_j) \Pi\mathbf{u}(\mathbf{r}_j) \cdot \mathbf{v}(\mathbf{r}_j) \\
&= \frac{1}{2} \sum_{j=1}^{4} |T_j| \hat{\mathbf{K}}^{-1}(\hat{\mathbf{r}}_j) \left(\frac{1}{J_e} \mathbf{DF}_e \hat{\Pi}\hat{\mathbf{u}} \right) (\hat{\mathbf{r}}_j) \cdot \left(\frac{1}{J_e} \mathbf{DF}_e \hat{\mathbf{v}} \right) (\hat{\mathbf{r}}_j) \\
&= \frac{1}{2} \sum_{j=1}^{4} \frac{|T_j|}{J_e(\hat{\mathbf{r}}_j)} \frac{1}{J_e(\hat{\mathbf{r}}_j)} \mathbf{DF}_e^T(\hat{\mathbf{r}}_j) \hat{\mathbf{K}}^{-1}(\hat{\mathbf{r}}_j) \mathbf{DF}_e(\hat{\mathbf{r}}_j)\, \hat{\Pi}\hat{\mathbf{u}}(\hat{\mathbf{r}}_j) \cdot \hat{\mathbf{v}}(\hat{\mathbf{r}}_j) \\
&= \frac{1}{4} \sum_{j=1}^{4} \mathbf{B}_e(\hat{\mathbf{r}}_j)\, \hat{\Pi}\hat{\mathbf{u}}(\hat{\mathbf{r}}_j) \cdot \hat{\mathbf{v}}(\hat{\mathbf{r}}_j) \\
&\equiv (\mathbf{B}_e \hat{\Pi}\hat{\mathbf{u}}, \hat{\mathbf{v}})_T,
\end{aligned}
$$

where the subscript T denotes the trapezoidal rule on element $\hat{e}$ and we define $\mathbf{B}_e = \frac{1}{J_e}\mathbf{DF}_e^T \hat{\mathbf{K}}^{-1}\mathbf{DF}_e$. Here we used (2.6) to conclude that $\frac{|T_j|}{J_e(\hat{\mathbf{r}}_j)} = \frac{1}{2}$. Considering the first term on the right-hand side of (4.18), we obtain

$$
\begin{aligned}
\int_e \mathbf{K}^{-1}\Pi\mathbf{u} \cdot \mathbf{v}\, d\mathbf{x} &= \int_{\hat{e}} \hat{\mathbf{K}}^{-1} \frac{1}{J_e} \mathbf{DF}_e \hat{\Pi}\hat{\mathbf{u}} \cdot \frac{1}{J_e} \mathbf{DF}_e \hat{\mathbf{v}} J_e\, d\hat{\mathbf{x}} \\
(4.20) &= \int_{\hat{e}} \frac{1}{J_e} \mathbf{DF}_e^T \hat{\mathbf{K}}^{-1} \mathbf{DF}_e \hat{\Pi}\hat{\mathbf{u}} \cdot \hat{\mathbf{v}}\, d\hat{\mathbf{x}} \\
&= \int_{\hat{e}} \mathbf{B}_e \hat{\Pi}\hat{\mathbf{u}} \cdot \hat{\mathbf{v}}\, d\hat{\mathbf{x}}.
\end{aligned}
$$

Substituting (4.19) and (4.20) into (4.18), we obtain

$$
(4.21) \qquad \sigma_e(\mathbf{K}^{-1}\Pi\mathbf{u}, \mathbf{v}) = \int_{\hat{e}} \mathbf{B}_e \hat{\Pi}\hat{\mathbf{u}} \cdot \hat{\mathbf{v}}\, d\hat{\mathbf{x}} - \left(\mathbf{B}_e \hat{\Pi}\hat{\mathbf{u}}, \hat{\mathbf{v}} \right)_T \equiv \sigma_{\hat{e}}\left(\mathbf{B}_e \hat{\Pi}\hat{\mathbf{u}}, \hat{\mathbf{v}} \right).
$$

Hereafter we shall omit the subscripts e and $\hat{e}$. Let

$$E(f) \equiv \int_{\hat{e}} f(\hat{x}, \hat{y}) d\hat{x}\, d\hat{y} - (f)_T$$

be the error of the trapezoidal rule for integrating a function $f(\hat{x}, \hat{y})$ on $\hat{e}$. Then,

$$(4.22) \qquad \sigma(\mathbf{B}\hat{\Pi}\hat{\mathbf{u}}, \hat{\mathbf{v}}) = E\big((\mathbf{B}\hat{\Pi}\hat{\mathbf{u}})_1 \hat{v}_1\big) + E\big((\mathbf{B}\hat{\Pi}\hat{\mathbf{u}})_2 \hat{v}_2\big).$$

We next bound the first term on the right-hand side in (4.22). The argument for the bound on the second term is similar.

Using the trapezoidal rule error representation from Lemma A.1 based on the Peano kernel theorem (see [23, Theorem 5.2-3, p. 142]), we write

$$
\begin{aligned}
E((\mathbf{B}\hat{\Pi}\hat{\mathbf{u}})_1 \hat{v}_1) &= \int_0^1 \int_0^1 \phi(\hat{x}) \frac{\partial^2}{\partial \hat{x}^2} \big((\mathbf{B}\hat{\Pi}\hat{\mathbf{u}})_1 \hat{v}_1\big)(\hat{x}, 0)\, d\hat{x}\, d\hat{y} \\
&\quad + \int_0^1 \int_0^1 \phi(\hat{y}) \frac{\partial^2}{\partial \hat{y}^2} (\mathbf{B}\hat{\Pi}\hat{\mathbf{u}})_1(0, \hat{y}) \hat{v}_1(0, \hat{y})\, d\hat{x}\, d\hat{y} \\
&\quad + \int_0^1 \int_0^1 \psi(\hat{x}, \hat{y}) \frac{\partial^2}{\partial \hat{x} \partial \hat{y}} \big((\mathbf{B}\hat{\Pi}\hat{\mathbf{u}})_1 \hat{v}_1\big)(\hat{x}, \hat{y})\, d\hat{x}\, d\hat{y} \\
&\equiv (I) + (II) + (III),
\end{aligned}
$$
(4.23)

where $\phi(t) = t(t-1)/2$ and $\psi(s, t) = (1-s)(1-t) - 1/4$. Denote by B_{11}, B_{12}, B_{21}, and B_{22} the components of the tensor $\mathbf{B}$. Since $\hat{v}_1(0, \hat{y})$ is constant in $\hat{y}$, the second term in (4.23) is

$$
\begin{aligned}
(II) &= \int_0^1 \int_0^1 \phi(\hat{y}) \frac{\partial^2}{\partial \hat{y}^2} B_{11}(0, \hat{y}) (\hat{\Pi}\hat{\mathbf{u}})_1(0, \hat{y}) \hat{v}_1(0, \hat{y})\, d\hat{x}\, d\hat{y} \\
&\quad + \int_0^1 \int_0^1 \phi(\hat{y}) \frac{\partial^2}{\partial \hat{y}^2} B_{12}(0, \hat{y}) (\hat{\Pi}\hat{\mathbf{u}})_2(0, \hat{y}) \hat{v}_1(0, \hat{y})\, d\hat{x}\, d\hat{y} \\
&\quad + 2 \int_0^1 \int_0^1 \phi(\hat{y}) \frac{\partial}{\partial \hat{y}} B_{12}(0, \hat{y}) \frac{\partial}{\partial \hat{y}} (\hat{\Pi}\hat{\mathbf{u}})_2(0, \hat{y}) \hat{v}_1(0, \hat{y})\, d\hat{x}\, d\hat{y} \\
&\equiv (II)_1 + (II)_2 + (II)_3.
\end{aligned}
$$
(4.24)

Using (4.8), for the first two terms on the right-hand side, we have

$$|(II)_1| + |(II)_2| \le C |\mathbf{B}|_{2,\infty,\hat{e}} \|\hat{\mathbf{u}}\|_{1,\hat{e}} \|\hat{v}_1\|_{\hat{e}}.$$

Since $\frac{\partial}{\partial \hat{y}} (\hat{\Pi}\hat{\mathbf{u}})_2$ is a constant, we rewrite the last term in (4.24) as

$$
\begin{aligned}
(II)_3 &= 2 \int_0^1 \int_0^1 \phi(\hat{y}) \frac{\partial}{\partial \hat{y}} B_{12}(0, \hat{y}) \frac{\partial}{\partial \hat{y}} (\hat{\Pi}\hat{\mathbf{u}})_2(\hat{x}, \hat{y}) \hat{v}_1(0, \hat{y})\, d\hat{x}\, d\hat{y} \\
&\le C |\mathbf{B}|_{1,\infty,\hat{e}} \left\| \frac{\partial}{\partial \hat{y}} (\hat{\Pi}\hat{\mathbf{u}})_2 \right\|_{\hat{e}} \|\hat{v}_1\|_{\hat{e}} \le C |\mathbf{B}|_{1,\infty,\hat{e}} |\hat{\mathbf{u}}|_{1,\hat{e}} \|\hat{v}_1\|_{\hat{e}},
\end{aligned}
$$

using (4.7). A combination of the last two bounds implies that

$$(4.25) \qquad |(II)| \le C\big(|\mathbf{B}|_{2,\infty,\hat{e}} \|\hat{\mathbf{u}}\|_{1,\hat{e}} + |\mathbf{B}|_{1,\infty,\hat{e}} |\hat{\mathbf{u}}|_{1,\hat{e}}\big) \|\hat{v}_1\|_{\hat{e}}.$$

For the last term in (4.23), since $\hat{v}_1(\hat{x}, \hat{y})$ is constant in $\hat{y}$, we have

$$(4.26) \quad (III) = \int_0^1 \int_0^1 \psi(\hat{x}, \hat{y}) \frac{\partial^2}{\partial \hat{x} \partial \hat{y}} (\mathbf{B}\hat{\Pi}\hat{\mathbf{u}})_1(\hat{x}, \hat{y}) \hat{v}_1(\hat{x}, \hat{y}) \, d\hat{x} \, d\hat{y}$$
$$+ \int_0^1 \int_0^1 \psi(\hat{x}, \hat{y}) \frac{\partial}{\partial \hat{y}} (\mathbf{B}\hat{\Pi}\hat{\mathbf{u}})_1(\hat{x}, \hat{y}) \frac{\partial}{\partial \hat{x}} \hat{v}_1(\hat{x}, \hat{y}) \, d\hat{x} \, d\hat{y} \equiv (III)_1 + (III)_2.$$

Using (4.7),

$$(4.27) \qquad |(III)_1| \leq C(|\mathbf{B}|_{2,\infty,\hat{e}} \|\hat{\mathbf{u}}\|_{1,\hat{e}} + |\mathbf{B}|_{1,\infty,\hat{e}} |\hat{\mathbf{u}}|_{1,\hat{e}}) \|\hat{v}_1\|_{\hat{e}}.$$

To bound $(III)_2$ we note that $\frac{\partial}{\partial \hat{x}} \hat{v}_1(\hat{x}, \hat{y})$ is a constant and $\int_0^1 \int_0^1 \psi(\hat{x}, \hat{y}) \, d\hat{x} \, d\hat{y} = 0$. Therefore, by the Bramble–Hilbert lemma [5], and using (4.7),

$$(4.28) \quad |(III)_2| \leq C \left| \frac{\partial}{\partial \hat{y}} (\mathbf{B}\hat{\Pi}\hat{\mathbf{u}})_1 \right|_{1,\hat{e}} \|\hat{v}_1\|_{\hat{e}} \leq C(|\mathbf{B}|_{2,\infty,\hat{e}} \|\hat{\mathbf{u}}\|_{1,\hat{e}} + |\mathbf{B}|_{1,\infty,\hat{e}} |\hat{\mathbf{u}}|_{1,\hat{e}}) \|\hat{v}_1\|_{\hat{e}}.$$

The first term in the error representation (4.23) is

$$(4.29) \qquad (I) = \int_0^1 \int_0^1 \phi(\hat{x}) \frac{\partial^2}{\partial \hat{x}^2} (\mathbf{B}\hat{\Pi}\hat{\mathbf{u}})_1(\hat{x}, 0) \, \hat{v}_1(\hat{x}, 0) \, d\hat{x} \, d\hat{y}$$
$$+ 2 \int_0^1 \int_0^1 \phi(\hat{x}) \frac{\partial}{\partial \hat{x}} (\mathbf{B}\hat{\Pi}\hat{\mathbf{u}})_1(\hat{x}, 0) \frac{\partial}{\partial \hat{x}} \hat{v}_1(\hat{x}, 0) \, d\hat{x} \, d\hat{y} = (I)_1 + (I)_2.$$

The first term on the right-hand side can be bounded in a way similar to (II):

$$(4.30) \qquad |(I)_1| \leq C(|\mathbf{B}|_{2,\infty,\hat{e}} \|\hat{\mathbf{u}}\|_{1,\hat{e}} + |\mathbf{B}|_{1,\infty,\hat{e}} |\hat{\mathbf{u}}|_{1,\hat{e}}) \|\hat{v}_1\|_{\hat{e}}.$$

We rewrite the second term on the right-hand side in (4.29) as

$$(4.31)$$
$$\frac{1}{2}(I)_2 = \int_0^1 \int_0^1 \phi(\hat{x}) \left(\frac{\partial}{\partial \hat{x}} (\mathbf{B}\hat{\Pi}\hat{\mathbf{u}})_1(\hat{x}, 0) - \frac{\partial}{\partial \hat{x}} (\mathbf{B}\hat{\Pi}\hat{\mathbf{u}})_1(\hat{x}, \hat{y}) \right) \frac{\partial}{\partial \hat{x}} \hat{v}_1(\hat{x}, 0) \, d\hat{x} \, d\hat{y}$$
$$+ \int_0^1 \int_0^1 \phi(\hat{x}) \frac{\partial}{\partial \hat{x}} (\mathbf{B}\hat{\Pi}\hat{\mathbf{u}})_1(\hat{x}, \hat{y}) \frac{\partial}{\partial \hat{x}} \hat{v}_1(\hat{x}, 0) \, d\hat{x} \, d\hat{y} \equiv (I)_{2,1} + (I)_{2,2}.$$

To estimate the first term in (4.31), we write

$$\frac{\partial}{\partial \hat{x}} (\mathbf{B}\hat{\Pi}\hat{\mathbf{u}})_1(\hat{x}, \hat{y}) - \frac{\partial}{\partial \hat{x}} (\mathbf{B}\hat{\Pi}\hat{\mathbf{u}})_1(\hat{x}, 0) = \int_0^{\hat{y}} \frac{\partial^2}{\partial \hat{x} \partial \hat{y}} (\mathbf{B}\hat{\Pi}\hat{\mathbf{u}})_1(\hat{x}, \hat{t}) \, d\hat{t}.$$

This allows us to bound the first term in (4.31) in a way similar to bounds (4.25) and (4.30):

$$(4.32) \qquad |(I)_{2,1}| \leq C(|\mathbf{B}|_{2,\infty,\hat{e}} \|\hat{\mathbf{u}}\|_{1,\hat{e}} + |\mathbf{B}|_{1,\infty,\hat{e}} |\hat{\mathbf{u}}|_{1,\hat{e}}) \|\hat{v}_1\|_{\hat{e}}.$$

The second term on the right-hand side in (4.31) can be rewritten as

$$(4.33) \quad (I)_{2,2} = \int_0^1 \int_0^1 \phi(\hat{x}) \frac{\partial}{\partial \hat{x}} (\mathbf{B}(\hat{\Pi}\hat{\mathbf{u}} - \hat{\mathbf{u}}))_1(\hat{x}, \hat{y}) \frac{\partial}{\partial \hat{x}} \hat{v}_1(\hat{x}, \hat{y}) \, d\hat{x} \, d\hat{y}$$
$$+ \int_0^1 \int_0^1 \phi(\hat{x}) \frac{\partial}{\partial \hat{x}} (\mathbf{B}\hat{\mathbf{u}})_1(\hat{x}, \hat{y}) \frac{\partial}{\partial \hat{x}} \hat{v}_1(\hat{x}, \hat{y}) \, d\hat{x} \, d\hat{y} \equiv (I)_{2,2,1} + (I)_{2,2,2},$$

where we used that $\frac{\partial}{\partial \hat{x}} \hat{v}_1(\hat{x}, 0) = \frac{\partial}{\partial \hat{x}} \hat{v}_1(\hat{x}, \hat{y})$ on e, since $\hat{v}_1$ is a constant in $\hat{y}$.

To estimate the second term in (4.33), we use the identity

$$(4.34) \qquad \frac{\partial}{\partial \hat{x}} \hat{v}_1 = -\frac{\partial}{\partial \hat{y}} \hat{v}_2 + \widehat{\operatorname{div}} \hat{\mathbf{v}}.$$

We rewrite $(I)_{2,2,2}$ as

$$(4.35)$$

$$\begin{aligned} (I)_{2,2,2} &= -\int_0^1 \int_0^1 \phi(\hat{x}) \frac{\partial}{\partial \hat{x}} (\mathbf{B}\hat{\mathbf{u}})_1 \frac{\partial}{\partial \hat{y}} \hat{v}_2 \, d\hat{x} \, d\hat{y} + \int_0^1 \int_0^1 \phi(\hat{x}) \frac{\partial}{\partial \hat{x}} (\mathbf{B}\hat{\mathbf{u}})_1 \widehat{\operatorname{div}} \hat{\mathbf{v}} \, d\hat{x} \, d\hat{y} \\ &= \int_{\hat{\ell}_1} - \int_{\hat{\ell}_3} \phi(\hat{x}) \frac{\partial}{\partial \hat{x}} (\mathbf{B}\hat{\mathbf{u}})_1 \hat{v}_2 \, d\hat{x} + \int_0^1 \int_0^1 \phi(\hat{x}) \frac{\partial^2}{\partial \hat{x} \partial \hat{y}} (\mathbf{B}\hat{\mathbf{u}})_1 \hat{v}_2 \, d\hat{x} \, d\hat{y} \\ &\quad + \int_0^1 \int_0^1 \phi(\hat{x}) \frac{\partial}{\partial \hat{x}} (\mathbf{B}\hat{\mathbf{u}})_1 \widehat{\operatorname{div}} \hat{\mathbf{v}} \, d\hat{x} \, d\hat{y}. \end{aligned}$$

Clearly, the last two terms can be bounded by

$$(4.36) \qquad C(|(\mathbf{B}\hat{\mathbf{u}})_1|_{2,\hat{e}} \|\hat{v}_2\|_{\hat{e}} + |(\mathbf{B}\hat{\mathbf{u}})_1|_{1,\hat{e}} \|\widehat{\operatorname{div}} \hat{\mathbf{v}}\|_{\hat{e}}).$$

We postpone the estimate of the edge integrals in (4.35) for later.

To bound the first term on the right-hand side in (4.33), we have

$$(4.37)$$

$$\begin{aligned} (I)_{2,2,1} &= \int_0^1 \int_0^1 \phi(\hat{x}) \frac{\partial}{\partial \hat{x}} B_{11}(\hat{x}, \hat{y}) (\hat{\Pi}\hat{\mathbf{u}} - \hat{\mathbf{u}})_1(\hat{x}, \hat{y}) \frac{\partial}{\partial \hat{x}} \hat{v}_1(\hat{x}, \hat{y}) \, d\hat{x} \, d\hat{y} \\ &\quad + \int_0^1 \int_0^1 \phi(\hat{x}) B_{11}(\hat{x}, \hat{y}) \frac{\partial}{\partial \hat{x}} (\hat{\Pi}\hat{\mathbf{u}} - \hat{\mathbf{u}})_1(\hat{x}, \hat{y}) \frac{\partial}{\partial \hat{x}} \hat{v}_1(\hat{x}, \hat{y}) \, d\hat{x} \, d\hat{y} \\ &\quad + \int_0^1 \int_0^1 \phi(\hat{x}) \frac{\partial}{\partial \hat{x}} B_{12}(\hat{x}, \hat{y}) (\hat{\Pi}\hat{\mathbf{u}} - \hat{\mathbf{u}})_2(\hat{x}, \hat{y}) \frac{\partial}{\partial \hat{x}} \hat{v}_1(\hat{x}, \hat{y}) \, d\hat{x} \, d\hat{y} \\ &\quad + \int_0^1 \int_0^1 \phi(\hat{x}) B_{12}(\hat{x}, \hat{y}) \frac{\partial}{\partial \hat{x}} (\hat{\Pi}\hat{\mathbf{u}} - \hat{\mathbf{u}})_2(\hat{x}, \hat{y}) \frac{\partial}{\partial \hat{x}} \hat{v}_1(\hat{x}, \hat{y}) \, d\hat{x} \, d\hat{y} \\ &\equiv (I)_{2,2,1,1} + (I)_{2,2,1,2} + (I)_{2,2,1,3} + (I)_{2,2,1,4}. \end{aligned}$$

Since $\hat{\Pi}\hat{\mathbf{u}}$ is exact for constants, using the Bramble–Hilbert lemma and the inverse inequality, we can bound the first and the third terms in (4.37) as

$$(4.38) \qquad |(I)_{2,2,1,1}| + |(I)_{2,2,1,3}| \le C|\mathbf{B}|_{1,\infty,\hat{e}} |\hat{\mathbf{u}}|_{1,\hat{e}} \|\hat{v}_1\|_{\hat{e}}.$$

For the second term in (4.37), a Taylor expansion of B_{11} about any fixed point $(\hat{x}_0, \hat{y}_0) \in \hat{e}$ gives

$$(4.39) \quad (I)_{2,2,1,2} = \int_0^1 \int_0^1 \phi(\hat{x}) B_{11}(\hat{x}_0, \hat{y}_0) \frac{\partial}{\partial \hat{x}} (\hat{\Pi}\hat{\mathbf{u}} - \hat{\mathbf{u}})_1(\hat{x}, \hat{y}) \frac{\partial}{\partial \hat{x}} \hat{v}_1(\hat{x}, \hat{y}) \, d\hat{x} \, d\hat{y} + R,$$

where

$$(4.40) \qquad |R| \le C|\mathbf{B}|_{1,\infty,\hat{e}} |\hat{\mathbf{u}}|_{1,\hat{e}} \|\hat{v}_1\|_{\hat{e}},$$

using (4.7) for the last inequality. To bound the first term on the right-hand side in (4.39), we note that

$$(\phi^2)''(\hat{x}) = 6\phi(\hat{x}) + \frac{1}{2}, \quad (\phi^2)'(0) = (\phi^2)'(1) = 0.$$

Therefore, using (4.6), we have

$$\int_0^1 \int_0^1 \phi(\hat{x}) B_{11}(\hat{x}_0, \hat{y}_0) \frac{\partial}{\partial \hat{x}} (\hat{\Pi}\hat{\mathbf{u}} - \hat{\mathbf{u}})_1(\hat{x}, \hat{y}) \frac{\partial}{\partial \hat{x}} \hat{v}_1(\hat{x}, \hat{y}) \, d\hat{x} \, d\hat{y}$$

(4.41)
$$= \frac{1}{6} \int_0^1 \int_0^1 \frac{\partial^2}{\partial \hat{x}^2} (\phi^2)(\hat{x}) B_{11}(\hat{x}_0, \hat{y}_0) \frac{\partial}{\partial \hat{x}} (\hat{\Pi}\hat{\mathbf{u}} - \hat{\mathbf{u}})_1(\hat{x}, \hat{y}) \frac{\partial}{\partial \hat{x}} \hat{v}_1(\hat{x}, \hat{y}) \, d\hat{x} \, d\hat{y}$$

$$= -\frac{1}{6} \int_0^1 \int_0^1 \frac{\partial}{\partial \hat{x}} (\phi^2)(\hat{x}) B_{11}(\hat{x}_0, \hat{y}_0) \frac{\partial^2}{\partial \hat{x}^2} (\hat{\Pi}\hat{\mathbf{u}} - \hat{\mathbf{u}})_1(\hat{x}, \hat{y}) \frac{\partial}{\partial \hat{x}} \hat{v}_1(\hat{x}, \hat{y}) \, d\hat{x} \, d\hat{y}$$

$$\leq C |\mathbf{B}|_{\infty, \hat{e}} |\hat{\mathbf{u}}|_{2, \hat{e}} \|\hat{v}_1\|_{\hat{e}}.$$

A combination of (4.39)–(4.41) gives

(4.42) $$|(I)_{2,2,1,2}| \leq C(|\mathbf{B}|_{1,\infty,\hat{e}} |\hat{\mathbf{u}}|_{1,\hat{e}} + |\mathbf{B}|_{\infty,\hat{e}} |\hat{\mathbf{u}}|_{2,\hat{e}}) \|\hat{v}_1\|_{\hat{e}}.$$

To complete the estimate of $(I)_{2,2,1}$, it remains to bound $(I)_{2,2,1,4}$. Using that $\frac{\partial}{\partial \hat{x}} (\hat{\Pi}\hat{\mathbf{u}})_2 = 0$ and (4.34), we have

(4.43)

$$(I)_{2,2,1,4} = \int_0^1 \int_0^1 \phi(\hat{x}) B_{12} \frac{\partial}{\partial \hat{x}} \hat{u}_2 \frac{\partial}{\partial \hat{y}} \hat{v}_2 \, d\hat{x} \, d\hat{y} - \int_0^1 \int_0^1 \phi(\hat{x}) B_{12} \frac{\partial}{\partial \hat{x}} \hat{u}_2 \, \widehat{\operatorname{div} \hat{\mathbf{v}}} \, d\hat{x} \, d\hat{y}$$

$$= \int_{\hat{\ell}_3} - \int_{\hat{\ell}_1} \phi(\hat{x}) \, B_{12} \frac{\partial}{\partial \hat{x}} \hat{u}_2 \, \hat{v}_2 \, d\hat{x} - \int_0^1 \int_0^1 \phi(\hat{x}) \frac{\partial}{\partial \hat{y}} \left(B_{12} \frac{\partial}{\partial \hat{x}} \hat{u}_2 \right) \hat{v}_2 \, d\hat{x} \, d\hat{y}$$

$$- \int_0^1 \int_0^1 \phi(\hat{x}) B_{12} \frac{\partial}{\partial \hat{x}} \hat{u}_2 \, \widehat{\operatorname{div} \hat{\mathbf{v}}} \, d\hat{x} \, d\hat{y}.$$

The last two terms above are bounded by

(4.44) $$C[(|\mathbf{B}|_{1,\infty,\hat{e}} |\hat{\mathbf{u}}|_{1,\hat{e}} + |\mathbf{B}|_{\infty,\hat{e}} |\hat{\mathbf{u}}|_{2,\hat{e}}) \|\hat{v}_2\|_{\hat{e}} + |\mathbf{B}|_{\infty,\hat{e}} |\hat{\mathbf{u}}|_{1,\hat{e}} \|\widehat{\operatorname{div} \hat{\mathbf{v}}}\|_{\hat{e}}].$$

Combining (4.23)–(4.44), we obtain

(4.45) $$E((\mathbf{B}\hat{\Pi}\hat{\mathbf{u}})_1 \hat{v}_1) = T_1 + T_2 + T_3,$$

where

(4.46) $$|T_1| \leq C[(|\mathbf{B}|_{2,\infty,\hat{e}} \|\hat{\mathbf{u}}\|_{1,\hat{e}} + |\mathbf{B}|_{1,\infty,\hat{e}} |\hat{\mathbf{u}}|_{1,\hat{e}} + |\mathbf{B}|_{\infty,\hat{e}} |\hat{\mathbf{u}}|_{2,\hat{e}}) \|\hat{\mathbf{v}}\|_{\hat{e}}$$
$$+ (|\mathbf{B}|_{1,\infty,\hat{e}} |\hat{\mathbf{u}}|_{\hat{e}} + |\mathbf{B}|_{\infty,\hat{e}} |\hat{\mathbf{u}}|_{1,\hat{e}}) \|\widehat{\operatorname{div} \hat{\mathbf{v}}}\|_{\hat{e}}],$$

(4.47) $$T_2 = \int_{\hat{\ell}_1} - \int_{\hat{\ell}_3} \phi(\hat{x}) \frac{\partial}{\partial \hat{x}} (\mathbf{B}\hat{\mathbf{u}})_1(\hat{x}, \hat{y}) \, \hat{v}_2(\hat{x}, \hat{y}) \, d\hat{x},$$

and

$$T_3 = \int_{\hat{\ell}_3} - \int_{\hat{\ell}_1} \phi(\hat{x}) \, B_{12}(\hat{x}, \hat{y}) \frac{\partial}{\partial \hat{x}} \hat{u}_2(\hat{x}, \hat{y}) \hat{v}_2(\hat{x}, \hat{y}) \, d\hat{x}.$$

Using Lemma 4.4 below, T_1 can be bounded as follows:

(4.48)
$$|T_1| \leq C \left[\left(h^2 \|\mathbf{K}^{-1}\|_{2,\infty,e} \|\mathbf{u}\|_{1,e} + h \|\mathbf{K}^{-1}\|_{1,\infty,e} h |\mathbf{u}|_{1,e} + \|\mathbf{K}^{-1}\|_{\infty,e} h^2 |\mathbf{u}|_{2,e} \right) \|\hat{\mathbf{v}}\|_{\hat{e}} \right.$$
$$\left. + \left(h \|\mathbf{K}^{-1}\|_{1,\infty,e} \|\mathbf{u}\|_{e} + \|\mathbf{K}^{-1}\|_{\infty,e} h \|\mathbf{u}\|_{1,e} \right) h \|\operatorname{div} \mathbf{v}\|_{e} \right]$$
$$\leq C h^2 \left(\|\mathbf{K}^{-1}\|_{2,\infty,e} \|\mathbf{u}\|_{2,e} \|\mathbf{v}\|_{e} + \|\mathbf{K}^{-1}\|_{1,\infty,e} \|\mathbf{u}\|_{1,e} \|\operatorname{div} \mathbf{v}\|_{e} \right),$$

using the fact that $|\hat{\mathbf{u}}|_{j,\hat{e}} \leq C h^j \|\mathbf{u}\|_{j,e}$ and $\|\widehat{\operatorname{div} \hat{\mathbf{v}}}\|_{\hat{e}} \leq C h \|\operatorname{div} \mathbf{v}\|_e$ (see [13, Lemma 5.5]).

The term $\sum_e T_2$ is treated in Lemma 4.5 below.

Finally, term T_3 in (4.45) can be rewritten as

$$T_3 = \int_{\hat{\ell}_3} - \int_{\hat{\ell}_1} \phi(\hat{s}) \, B_{12}(\hat{s}, \hat{y}) \frac{\partial}{\partial \hat{s}} (\hat{\mathbf{u}} \cdot \hat{\mathbf{n}}_k) \hat{\mathbf{v}} \cdot \hat{\mathbf{n}}_k \, d\hat{s}.$$

A similar term appears in the proof of Theorem 5.1 in [13]. Following the argument there, it can be shown that

$$(4.49) \qquad \left| \sum_e T_3 \right| \leq C \sum_e h^2 \|\mathbf{u}\|_{2,e} \|\mathbf{v}\|_e.$$

A combination of estimates (4.45), (4.48), (4.51), and (4.49) implies that

$$\sum_e |E((\mathbf{B}\hat{\Pi}\hat{\mathbf{u}})_1 \hat{v}_1)| \leq C h^2 (\|\mathbf{u}\|_2 \|\mathbf{v}\| + \|\mathbf{u}\|_1 \|\operatorname{div} \mathbf{v}\|).$$

The argument for $E((\mathbf{B}\hat{\Pi}\hat{\mathbf{u}})_2 \hat{v}_2)$ is analogous. This completes the proof of the lemma.   □

We next give the proofs of the two auxiliary lemmas used in the above argument.

LEMMA 4.4.   *If* $\mathbf{K}^{-1} \in W^{2,\infty}(\Omega)$, *then for all* $e \in \mathcal{T}_h$ *there exists a positive constant* C *independent of* h *such that*

$$|\mathbf{B}|_{s,\infty,\hat{e}} \leq C \, h^s \, \|\mathbf{K}^{-1}\|_{s,\infty,e}, \qquad s = 0, 1, 2.$$

Proof. First, for a quasi-uniform mesh, we have

$$c_1 \, h \leq \|\mathbf{DF}\|_{\infty,\hat{e}} \leq c_2 \, h, \quad c_3 \, h^2 \leq \|J\|_{\infty,\hat{e}} \leq c_4 \, h^2$$

with some positive constants c_1–c_4. This implies that

$$(4.50) \qquad \|\mathbf{B}\|_{\infty,\hat{e}} \leq C \, \|\hat{\mathbf{K}}^{-1}\|_{\infty,\hat{e}}.$$

Second, for an h^2-uniform mesh, we have additional estimates. Let $\alpha = (\alpha_1, \alpha_2)$, $\alpha_i \geq 0$, be a double index, and let $|\alpha| = \alpha_1 + \alpha_2$. In the case $|\alpha| = 1$, the definition of the bilinear mapping (2.4)–(2.6) and (2.2) imply that

$$\|\hat{\partial}^\alpha \mathbf{DF}\|_{\infty,\hat{e}} \leq C \, h^2 \qquad \text{and} \qquad \left\| \hat{\partial}^\alpha \frac{1}{J} \mathbf{DF} \right\|_{\infty,\hat{e}} \leq C.$$

In the case $|\alpha| = 2$, we have the estimates

$$\|\hat{\partial}^\alpha \mathbf{DF}\|_{\infty,\hat{e}} = 0 \qquad \text{and} \qquad \left\| \hat{\partial}^\alpha \frac{1}{J} \mathbf{DF} \right\|_{\infty,\hat{e}} \leq C \, h.$$

As a result, we get

$$\|\hat{\partial}^\alpha \mathbf{B}\|_{\infty,\hat{e}} \leq C \, (h\|\hat{\mathbf{K}}^{-1}\|_{\infty,\hat{e}} + \|\hat{\partial}^\alpha \hat{\mathbf{K}}^{-1}\|_{\infty,\hat{e}})$$

for $|\alpha| = 1$ and

$$\|\hat{\partial}^\alpha \mathbf{B}\|_{\infty,\hat{e}} \leq C \, (h^2 \, \|\hat{\mathbf{K}}^{-1}\|_{\infty,\hat{e}} + h \, \|\hat{\partial}^{\alpha-1} \hat{\mathbf{K}}^{-1}\|_{\infty,\hat{e}} + \|\hat{\partial}^\alpha \hat{\mathbf{K}}^{-1}\|_{\infty,\hat{e}})$$

for $|\alpha| = 2$. Since $\hat{\mathbf{K}}^{-1} = \mathbf{K}^{-1} \circ \mathbf{F}$, using the chain rule and $\|\hat{\partial}^{\alpha}\mathbf{F}\|_{\infty,\hat{e}} \leq C\,h^{|\alpha|}$ for $|\alpha| \leq 2$, we obtain

$$\|\hat{\partial}^{\alpha}\hat{\mathbf{K}}^{-1}\|_{\infty,\hat{e}} \leq C\,h^{|\alpha|}\,\|\mathbf{K}^{-1}\|_{|\alpha|,\infty,e}, \quad |\alpha| = 0,1,2,$$

which implies

$$\|\hat{\partial}^{\alpha}\mathbf{B}\|_{\infty,\hat{e}} \leq C\,h^{|\alpha|}\,\|\mathbf{K}^{-1}\|_{|\alpha|,\infty,e}, \quad |\alpha| = 0,1,2,$$

completing the proof. $\square$

LEMMA 4.5. *If $\mathbf{K}^{-1} \in W^{2,\infty}(\Omega)$, then*

$$(4.51) \qquad \sum_e T_2 = 0,$$

where T_2 is defined in (4.47).

Proof. Summing over all elements in (4.47), we have

$$(4.52) \qquad \sum_e T_2 = \sum_e \sum_{k=1,3} \int_{\hat{\ell}_k} \phi(\hat{s})\,\frac{\partial}{\partial\hat{s}}((\mathbf{B}\hat{\mathbf{u}})\cdot\hat{\boldsymbol{\tau}}_k)\hat{\mathbf{v}}\cdot\hat{\mathbf{n}}_k\,d\hat{s}.$$

Using (2.7), we have that for any edge ℓ,

$$(\mathbf{B}\hat{\mathbf{u}})\cdot\hat{\boldsymbol{\tau}} = \frac{1}{J}\mathbf{DF}^T\hat{\mathbf{K}}^{-1}\mathbf{DF}\hat{\mathbf{u}}\cdot|\ell|\mathbf{DF}^{-1}\boldsymbol{\tau} = |\ell|(\mathbf{K}^{-1}\mathbf{u})\cdot\boldsymbol{\tau}.$$

Therefore, using (2.9), the sum in (4.52) becomes

$$(4.53) \qquad \sum_e T_2 = \sum_e \sum_{k=1,3} |\ell_k|^2 \int_{\ell_k} \phi(s)\,\frac{\partial}{\partial s}((\mathbf{K}^{-1}\mathbf{u})\cdot\boldsymbol{\tau}_k)\mathbf{v}\cdot\mathbf{n}_k\,ds.$$

Since $\mathbf{v} \in \mathbf{V}^h$, $\mathbf{v}\cdot\mathbf{n} = 0$ on exterior edges and $\mathbf{v}\cdot\mathbf{n}$ is continuous across interior edges. The assumed regularity for $\mathbf{K}$ and $\mathbf{u}$ implies that $\mathbf{K}^{-1}\mathbf{u}$ and $\frac{\partial}{\partial s}(\mathbf{K}^{-1}\mathbf{u})$ are continuous across interior edges. Note that each interior edge ℓ appears twice in the sum in (4.53), which now can be rewritten as a sum of interior edge integrals

$$\sum_e T_2 = \sum_\ell |\ell|^2 \int_\ell \phi(s)\,\frac{\partial}{\partial s}((\mathbf{K}^{-1}\mathbf{u})\cdot\boldsymbol{\tau})[\mathbf{v}\cdot\mathbf{n}]\,ds = 0,$$

where $[\mathbf{v}\cdot\mathbf{n}]$ denotes the jump in the normal component of $\mathbf{v}$. $\square$

5. Superconvergence to the average edge fluxes and at the edge midpoints. We now discuss how the superconvergence result from section 4 can be applied to obtain superconvergence for the computed velocity to the average edge fluxes and at the midpoints of the edges. Define, for any $\mathbf{v} \in (H^1(\Omega))^2$,

$$(5.1) \qquad \forall e \in \mathcal{T}_h, \quad |||\mathbf{v}|||_e^2 = \sum_{k=1}^{4} \left(\int_{\ell_k} \mathbf{v}\cdot\mathbf{n}_k\,ds\right)^2,$$

$$(5.2) \qquad |||\mathbf{v}|||^2 = \sum_{e\in\mathcal{T}_h} |||\mathbf{v}|||_e^2.$$

Using the well-known property of the Piola transformation [6],

$$(5.3) \qquad \int_\ell \mathbf{v} \cdot \mathbf{n} \, ds = \int_{\hat{\ell}} \hat{\mathbf{v}} \cdot \hat{\mathbf{n}} \, d\hat{s} \quad \forall \, \mathbf{v} \in (H^1(\Omega))^2,$$

and transforming to the reference element and back, it is easy to see that $||| \cdot |||$ is a norm on $\mathbf{V}^h$ and there exist constants c_1 and c_2 independent of h such that

$$c_1 \|\mathbf{v}\| \le |||\mathbf{v}||| \le c_2 \|\mathbf{v}\| \quad \forall \, \mathbf{v} \in \mathbf{V}^h.$$

It is clear from (4.2) and (5.3) that $|||\Pi\mathbf{v} - \mathbf{v}||| = 0$ for any $\mathbf{v} \in (H^1(\Omega))^2$. Therefore,

$$(5.4) \qquad |||\mathbf{u} - \mathbf{u}^h||| \le |||\Pi\mathbf{u} - \mathbf{u}^h||| \le c_2 \|\Pi\mathbf{u} - \mathbf{u}^h\| \le Ch^2 \|\mathbf{u}\|_2,$$

using Theorem 4.2. This implies edgewise superconvergence of the computed velocity $\mathbf{u}^h \cdot \mathbf{n}$ to $\frac{1}{|\ell|} \int_\ell \mathbf{u} \cdot \mathbf{n} \, ds$ in a discrete L^2-sense.

REMARK 5.1. *The superconvergence result (5.4) implies similar superconvergence for $|||\mathbf{u} - \mathbf{u}^h|||_M$ with*

$$|||\mathbf{v}|||_M^2 = \sum_{e \in \mathcal{T}_h} \sum_{k=1}^4 |\ell_k|^2 (\mathbf{v} \cdot \mathbf{n}_k)^2 (m_k),$$

where m_k is the midpoint of ℓ_k. Our choice of reporting the results in $||| \cdot |||$ is motivated by the fact that average fluxes are easier to measure than pointwise values and therefore are of greater practical interest.

6. Numerical experiments. In this section, we present the details of the numerical implementation. Instead of solving saddle point problem (2.10), we reduce it to an equivalent system with a symmetric positive definite matrix using the standard hybridization technique.

Let $\mathbf{V}_e^h$ be the restriction of $\mathbf{V}^h$ to quadrilateral e and Λ_ℓ^h be the space of constant functions over edge ℓ. Define

$$\tilde{\mathbf{V}}^h = \prod_e \mathbf{V}_e^h \quad \text{and} \quad \Lambda^h = \prod_\ell \Lambda_\ell^h.$$

Note that the normal component of $\mathbf{v}^h \in \mathbf{V}^h$ is continuous across interior mesh edges and $\mathbf{v}^h \cdot \mathbf{n} = 0$ on exterior edges. Therefore,

$$\mathbf{V}^h = \left\{ \tilde{\mathbf{v}}^h \in \tilde{\mathbf{V}}^h \colon \; \sum_e (\mu^h, \tilde{\mathbf{v}}^h \cdot \mathbf{n}_e)_{\partial e} = 0 \quad \forall \mu^h \in \Lambda^h \right\},$$

where $\mathbf{n}_e$ is the outward normal vector for quadrilateral e.

It has been shown by many authors (see, e.g., [6]) that the original formulation (2.10) is equivalent to the mixed-hybrid formulation: find $(\tilde{\mathbf{u}}^h, p^h, \lambda^h) \in \tilde{\mathbf{V}}^h \times W^h \times \Lambda^h$ such that

$$(6.1) \quad \begin{aligned} (\mathbf{K}^{-1}\tilde{\mathbf{u}}^h, \tilde{\mathbf{v}}^h)_{h,e} - (p^h, \operatorname{div} \tilde{\mathbf{v}}^h)_e + (\lambda^h, \tilde{\mathbf{v}}^h \cdot \mathbf{n}_e)_{\partial e} &= 0 & \forall \tilde{\mathbf{v}}^h \in \tilde{\mathbf{V}}^h, \\ (\operatorname{div} \tilde{\mathbf{u}}^h, w^h)_e &= (f, w^h)_e & \forall w^h \in W^h, \\ \sum_e (\mu^h, \tilde{\mathbf{u}}^h \cdot \mathbf{n}_e)_{\partial e} &= 0 & \forall \mu^h \in \Lambda^h. \end{aligned}$$

System (6.1) can be written in the matrix form as

(6.2)
$$\begin{pmatrix} M & B^T & C^T \\ B & 0 & 0 \\ C & 0 & 0 \end{pmatrix} \begin{pmatrix} u \\ p \\ \lambda \end{pmatrix} = \begin{pmatrix} 0 \\ f \\ 0 \end{pmatrix},$$

where

$$D = \begin{pmatrix} M & B^T \\ B & 0 \end{pmatrix}$$

is a block-diagonal matrix (after a permutation of columns and rows) with as many blocks as mesh elements. Each block is a 5×5 matrix. Therefore, vectors u and p can be explicitly eliminated from (6.2) resulting in a system

(6.3)
$$S \lambda = b,$$

where S is a sparse symmetric positive definite matrix. For logically rectangular meshes, S has at most seven nonzero elements in each row and column. Its nonzero entries represent connections between edge-based unknowns belonging to the same cell.

Problem (6.3) was solved with the preconditioned conjugate gradient (PCG) method. In the numerical experiments, we used one V-cycle of the algebraic multigrid method [24] as a preconditioner. The stopping criterion for the PCG method was the relative decrease in the norm of the residual by a factor of 10^{-12}.

We solved the boundary problem (1.1) with a known analytic solution

$$p(x, y) = x^3 y^2 + x \, \cos(xy) \, \sin(x)$$

and tensor coefficient

$$\mathbf{K}(x, y) = \begin{pmatrix} (x+1)^2 + y^2 & -xy \\ -xy & (x+1)^2 \end{pmatrix}.$$

It is pertinent to note here that the superconvergence result established in the previous section for the homogeneous Neumann boundary condition can be extended to the case of general Neumann boundary value problem.

In example 1, the computational domain Ω is the unit square. The computational grid is constructed from a uniform rectangular grid via the mapping

$$x(\xi, \eta) = \xi + 0.06 \, \sin(2\pi\eta) \, \sin(2\pi\xi), \qquad y(\xi, \eta) = \eta + 0.06 \, \sin(2\pi\eta) \, \sin(2\pi\xi),$$

where $0 < \eta, \xi < 1$, and subsequent random distortion of mesh node positions (see Figure 6.1). The maximum value of the distortion is proportional to the square of the local mesh size; i.e., the resulting grid satisfies assumptions (2.2) and (2.3). We test both Neumann and Dirichlet boundary conditions. The results for the Neumann problem are shown in Table 6.1. The convergence rates were computed using the linear regression for the data in the rows for $1/h = 32, 64, 128, 256$. In addition to norm (5.2), we show the convergence rate in the discrete L_∞-norm:

$$|||\mathbf{u} - \mathbf{u}^h|||_\infty = \max_{\ell_k} \left| \frac{1}{|\ell_k|} \int_{\ell_k} \mathbf{u} \cdot \mathbf{n}_k \, ds \ - \mathbf{u}^h \cdot \mathbf{n}_k \right|,$$
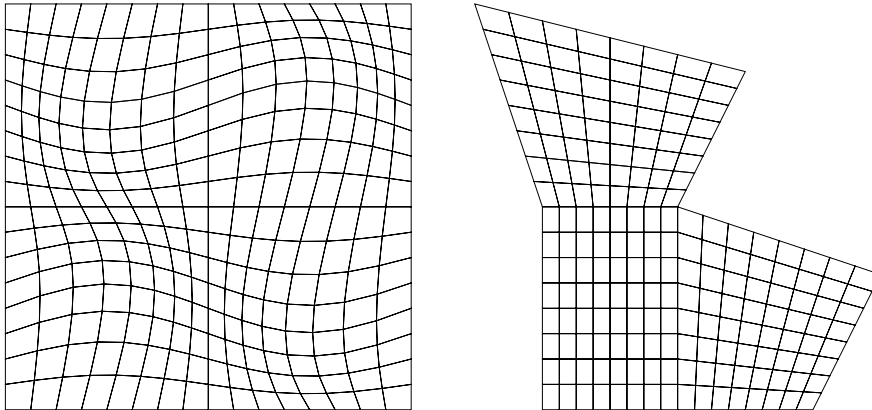
Fig. 6.1. *Examples of meshes used in numerical experiments.*

Table 6.1
Convergence rates for example 1: Neumann boundary conditions.

$1/h$	$\|\|\|\mathbf{u} - \mathbf{u}^h\|\|\|_\infty$	$\|\|\|\mathbf{u} - \mathbf{u}^h\|\|\|$	$\|\|\|p - p^h\|\|\|_\infty$	$\|\|\|p - p^h\|\|\|$
8	8.32e-2	5.47e-2	4.75e-3	1.45e-3
16	2.84e-2	1.69e-2	1.57e-3	3.99e-4
32	8.84e-3	4.49e-3	4.40e-4	1.03e-4
64	2.42e-3	1.14e-3	1.16e-4	2.59e-5
128	6.32e-4	2.87e-4	2.96e-5	6.48e-6
256	1.61e-4	7.17e-5	7.49e-6	1.62e-6
Rate	1.93	1.99	1.96	2.00

where the maximum is taken over all mesh edges. The convergence rates for the pressure variable are shown in the following discrete norms:

$$\|\|\|p - p^h\|\|\|^2 = \sum_{e_i \in \mathcal{T}_h} |p(c_i) - p^h(c_i)|^2 \, |e_i|$$

and

$$\|\|\|p - p^h\|\|\|_\infty = \max_{e_i \in \mathcal{T}_h} |p(c_i) - p^h(c_i)|,$$

where c_i is the geometric center of element e_i. The use of the geometric center instead of the mass center is due to the following property of the MFD method. The method is exact for linear solutions when the pressure variable, $p(c_i)$, is evaluated at the geometric center c_i [15]. The second-order convergence rate is observed for both the pressure and velocity variables in the discrete L_2- and L_∞-norms.

In the case of Dirichlet boundary conditions, a loss of one half order in the convergence rate for the velocity in the L_2-norm is expected (see, e.g., [12, 3]). The convergence rates are shown in Table 6.2. Note that the velocity convergence rate in the L_2-norm is larger than the theoretical bound of $O(h^{1.5})$. However, the convergence rate in the L_∞-norm is only $O(h)$.

In example 2, the computational domain Ω consists of three quadrilaterals (see Figure 6.1). A sequence of grids is obtained by uniform refinement of these quadrilaterals. The left bottom corner of the domain is located at the point $(1,0)$. The results

TABLE 6.2
Convergence rates for example 1: Dirichlet boundary conditions.

$1/h$	$\|\|\|\mathbf{u} - \mathbf{u}^h\|\|\|_\infty$	$\|\|\|\mathbf{u} - \mathbf{u}^h\|\|\|$	$\|\|\|p - p^h\|\|\|_\infty$	$\|\|\|p - p^h\|\|\|$
8	1.50e-1	8.58e-2	5.08e-3	2.08e-3
16	7.20e-2	2.59e-2	1.64e-3	5.53e-3
32	4.24e-2	6.97e-3	4.71e-4	1.42e-4
64	2.39e-2	1.81e-3	1.26e-4	3.57e-5
128	1.27e-2	4.65e-4	3.26e-5	8.95e-6
256	6.55e-3	1.19e-4	8.26e-6	2.24e-6
Rate	0.90	1.96	1.95	2.00

TABLE 6.3
Convergence rates for example 2: Neumann boundary conditions.

$1/h$	$\|\|\|\mathbf{u} - \mathbf{u}^h\|\|\|_\infty$	$\|\|\|\mathbf{u} - \mathbf{u}^h\|\|\|$	$\|\|\|p - p^h\|\|\|_\infty$	$\|\|\|p - p^h\|\|\|$
8	1.59e-1	1.08e-1	8.84e-3	5.05e-3
16	5.23e-2	2.79e-2	2.74e-3	1.21e-3
32	1.72e-2	7.07e-3	8.33e-4	2.95e-4
64	5.65e-3	1.78e-3	2.26e-4	7.30e-5
128	1.85e-3	4.45e-4	5.84e-5	1.82e-5
256	6.06e-4	1.11e-4	1.48e-5	4.53e-6
Rate	1.61	2.00	1.94	2.01

of our numerical experiments are shown in Table 6.3. We realize that the grid is only locally h^2-uniform. However, the second-order convergence rate for the velocity variable in the L_2 norm is attained.

7. Conclusion. We have proved the superconvergence estimate for the velocity variable on h^2-uniform quadrilateral grids when the exact integration of velocities is replaced by a novel 4-point quadrature rule. The theoretical results for the full diffusion tensor have been confirmed with numerical experiments.

Appendix. Representation of the trapezoidal rule error.
LEMMA A.1. *Let $f(x, y)$ be a function defined on a rectangular domain $[a, b] \times [c, d]$. The trapezoidal rule error*

$$E(f) \equiv \int_a^b \int_c^d f(x, y)\, dx\, dy - (f)_T$$

can be represented as

$$E(f) = (d - c) \int_a^b \frac{(x - a)(x - b)}{2} \frac{\partial^2}{\partial x^2} f(x, c)\, dx$$
$$+ (b - a) \int_c^d \frac{(y - c)(y - d)}{2} \frac{\partial^2}{\partial y^2} f(a, y)\, dy$$
$$+ \int_a^b \int_c^d \left((x - b)(y - d) - \frac{(b - a)(d - c)}{4} \right) \frac{\partial^2}{\partial x \partial y} f(x, y)\, dx\, dy.$$

Proof. Define a function

$$g^k(x, s) \equiv (x - s)_+^k \equiv \begin{cases} (x - s)^k, & x \geq s, \\ 0, & x < s, \end{cases}$$

where $k \geq 0$. The Peano kernel theorem (see [23, Theorem 5.2-3, p. 142]) states that the error of the trapezoidal rule is given by

$$E(f) = \int_a^b A_{2,0}(s) f^{(2,0)}(s,c)\, ds$$

(A.1)
$$+ \int_c^d A_{0,2}(t) f^{(0,2)}(a,t)\, dt$$

$$+ \int_a^b \int_c^d A_{1,1}(s,t) f^{(1,1)}(s,t)\, ds\, dt,$$

where $f^{(i,j)}(x,y) = \frac{\partial^{i+j}}{\partial x^i \partial y^j} f(x,y)$ for $i, j \geq 0$ and

$$A_{2,0}(s) = E(g^1(x,s)), \quad A_{0,2}(t) = E(g^1(y,t)), \quad A_{1,1}(s,t) = E(g^0(x,s)g^0(y,t)).$$

Straightforward calculations give

$$A_{2,0}(s) = \int_a^b \int_c^d g^1(s,x)\, dx\, dy - \frac{(b-a)(d-c)}{4} \sum_{j=1}^4 g(x_j,s)$$

(A.2)
$$= (d-c)\left(\int_s^b (x-s)\, dx - \frac{b-a}{2}\left(g(a,s) - g(b,s)\right)\right)$$

$$= (d-c)\frac{(s-a)(s-b)}{2}.$$

Similarly, we get

(A.3)
$$A_{0,2}(t) = (b-a)\frac{(t-c)(t-d)}{2} \quad \text{and} \quad A_{1,1}(s,t) = (s-b)(t-d) - \frac{(b-a)(d-c)}{4}.$$

A substitution of (A.2) and (A.3) into (A.1) completes the proof. $\quad\square$

REFERENCES

[1] T. ARBOGAST, L. C. COWSAR, M. F. WHEELER, AND I. YOTOV, *Mixed finite element methods on nonmatching multiblock grids,* SIAM J. Numer. Anal., 37 (2000), pp. 1295–1315.

[2] T. ARBOGAST, C. N. DAWSON, P. T. KEENAN, M. F. WHEELER, AND I. YOTOV, *Enhanced cell-centered finite differences for elliptic equations on general geometry,* SIAM J. Sci. Comput., 19 (1998), pp. 404–425.

[3] T. ARBOGAST, M. F. WHEELER, AND I. YOTOV, *Mixed finite elements for elliptic problems with tensor coefficients as cell-centered finite differences,* SIAM J. Numer. Anal., 34 (1997), pp. 828–852.

[4] M. BERNDT, K. LIPNIKOV, J. D. MOULTON, AND M. SHASHKOV, *Convergence of mimetic finite difference discretizations of the diffusion equation,* J. Numer. Math., 9 (2001), pp. 253–284.

[5] D. BRAESS, *Finite Elements: Theory, Fast Solvers, and Applications in Solid Mechanics,* Cambridge University Press, Cambridge, UK, 1997.

[6] F. BREZZI AND M. FORTIN, *Mixed and Hybrid Finite Element Methods,* Springer Ser. Comput. Math. 15, Springer-Verlag, New York, 1991.

[7] Z. CAI, J. E. JONES, S. F. MCCORMICK, AND T. F. RUSSELL, *Control-volume mixed finite element methods,* Comput. Geosci., 1 (1997), pp. 289–315.

[8] J. CAMPBELL AND M. SHASHKOV, *A tensor artificial viscosity using a mimetic finite difference algorithm,* J. Comput. Phys., 172 (2001), pp. 739–765.

[9] S.-H. CHOU, D. Y. KWAK, AND K. Y. KIM, *A general framework for constructing and analyzing mixed finite volume methods on quadrilateral grids: The overlapping covolume case,* SIAM J. Numer. Anal., 39 (2001), pp. 1170–1196.

[10] J. Douglas, Jr. and J. Wang, *Superconvergence for mixed finite element methods on rectangular domains,* Calcolo, 26 (1989), pp. 121–134.

[11] R. Durán, *Superconvergence for rectangular mixed finite element methods,* Numer. Math., 58 (1990), pp. 287–298.

[12] R. E. Ewing, R. D. Lazarov, and J. Wang, *Superconvergence of the velocity along the Gauss lines in mixed finite element methods,* SIAM J. Numer. Anal., 28 (1991), pp. 1015–1029.

[13] R. E. Ewing, M. Liu, and J. Wang, *Superconvergence of mixed finite element approximations over quadrilaterals,* SIAM J. Numer. Anal., 36 (1999), pp. 772–787.

[14] J. M. Hyman and M. Shashkov, *Mimetic discretizations for Maxwell's equations and the equations of magnetic diffusion,* Progr. Electromagn. Res., 32 (2001), pp. 89–121.

[15] J. M. Hyman, M. Shashkov, and S. Steinberg, *The numerical solution of diffusion problems in strongly heterogeneous non-isotropic materials,* J. Comput. Phys., 132 (1997), pp. 130–148.

[16] K. Lipnikov, J. Morel, and M. Shashkov, *Mimetic finite difference methods for diffusion equations on non-orthogonal AMR meshes,* J. Comput. Phys., 199 (2004), pp. 589–597.

[17] L. Margolin, M. Shashkov, and P. Smolarkiewicz, *A discrete operator calculus for finite difference approximations,* Comput. Methods Appl. Mech. Engrg., 187 (2000), pp. 365–383.

[18] J. E. Morel, R. M. Roberts, and M. Shashkov, *A local support-operators diffusion discretization scheme for quadrilateral $r-z$ meshes,* J. Comput. Phys., 144 (1998), pp. 17–51.

[19] M. Nakata, A. Weiser, and M. F. Wheeler, *Some superconvergence results for mixed finite element methods for elliptic problems on rectangular domains,* in The Mathematics of Finite Elements and Applications, V. J. Whiteman, ed., Academic Press, London, 1985.

[20] R. A. Raviart and J. M. Thomas, *A mixed finite element method for 2nd order elliptic problems,* in Mathematical Aspects of the Finite Element Method, Lecture Notes in Math. 606, Springer-Verlag, New York, 1977, pp. 292–315.

[21] T. F. Russell and M. F. Wheeler, *Finite element and finite difference methods for continuous flows in porous media,* in The Mathematics of Reservoir Simulation, Frontiers Appl. Math. 1, R. E. Ewing, ed., SIAM, Philadelphia, 1983, pp. 35–106.

[22] M. Shashkov and S. Steinberg, *Solving diffusion equations with rough coefficients in rough grids,* J. Comput. Phys., 129 (1996), pp. 383–405.

[23] A. H. Stroud, *Approximate Calculation of Multiple Integrals,* Prentice–Hall, Englewood Cliffs, NJ, 1971.

[24] K. Stüben, *Algebraic multigrid (AMG): Experiences and comparisons,* Appl. Math. Comput., 13 (1983), pp. 419–452.

[25] J. M. Thomas, *Sur l'analyse numérique des méthods d'éléments finis hybrides et mixtes,* Ph.D. thesis, Université Pierre et Marie Curie, Paris, 1977.

[26] J. Wang and T. P. Mathew, *Mixed finite element method over quadrilaterals,* in Conference on Adv. Numer. Methods and Appl., I. T. Dimov, B. Sendov, and P. Vassilevski, eds., World Scientific, River Edge, NJ, 1994, pp. 203–214.

[27] A. Weiser and M. F. Wheeler, *On convergence of block-centered finite-differences for elliptic problems,* SIAM J. Numer. Anal., 25 (1988), pp. 351–375.